Magnon Landau-Zener tunnelling and spin current generation by electric field

YuanDong Wang[1,2], Zhen-Gang Zhu[1,2,3,*] and Gang Su[2,3,4†]

[1] *School of Electronic, Electrical and Communication Engineering, University of Chinese Academy of Sciences, Beijing 100049, China.*

[2] *School of Physical Sciences, University of Chinese Academy of Sciences, Beijing 100049, China.*

[3] *CAS Center for Excellence in Topological Quantum Computation, University of Chinese Academy of Sciences, Beijing 100049, China.*

[4] *Kavli Institute for Theoretical Sciences, University of Chinese Academy of Sciences, Beijing 100190, China.*

To control the magnon transport in magnetic systems is of great interest in magnonics. Due to the feasibility of electric field, how to generate and manipulate magnon with pure electrical method is one of the most desired goals. Here we propose that the magnon spin current is generated by applying time-dependent electric field, where the coupling between the magnon and electric field is invoked via Aharonov-Casher effect. In particular, the magnon spin current is dominated by electric field component which perpendicular to the magnetization direction. We apply our theory to 1D ferromagnetic SSH model and show that the generated magnon spin current is closely related to the band geometry. Our findings expands the horizons of magnonics and electric-control-magnon mechanisms.

I. INTRODUCTION

Magnons, whose quanta are spin-1 spin waves, are the collective excitations of ordered magnets [1]. Very recently, magnon- based spintronics has attracted much attentions due to distinguish advantages of magnons. The charge neutrality, leading that spin current carried by magnons does not incur Joule heating, as well as the long coherence length, which hold huge potential to realize low-dissipation devices [2–6]. The creation and control of magnon spin currents at the nanoscale are key goals in spintronics and magnonics. Therefore, much effort has been focused on the thermal control on magnons [7–20]. However, the thermal control is not easily accurately controlled and sometimes even cumbersome. Consequently, a desired goal is to generate and control the magnon transport via electrical method. Nevertheless, owing to the charge neutrality, there is not a direct coupling between the magnons and the electric field, manifests itself as an elemental obstacle. Recently, increasing interest has been recently devoted to overcome this difficulty. For example, it has been proposed that the magnon spin current is generated by circularly polarized light via a two magnon Raman process [21]. The optical control of magnons is proposed making use of the magnetoelectric coupling in multiferroic materials, [22–24]. Particularly, the dc magnon spin photocurrents has been predicted recently in collinear antiferromagnets via the coupling between electric field and polarization with a broken inversion symmetry [25]. Noting that the dc magnon spin current is of difference frequency in response to electric field or magnetic field. It is regarded as a second-order term for which the signal could be relatively small compare to the linear response (when the linear response is finite). Therefore, it is interesting to investigate the magnon response to electric field including the linear-order.

Here we elucidate the characteristics of magnon spin currents in magnetic insulator materials, by leveraging Aharonov-Casher (AC) effect [26], a geometric phase the magnons pick along the path in the presence of electric field. We find that the effect of electric field perturbation is described by dipole interaction between the effective electric field and the magnon position that mediated by AC phase. By leveraging the obtained perturbation Hamiltonian we solve the time-dependent Schördinger for magnons which does not rely on a nonperturbative expansion on electric field. We find that the magnon spin current is determined by the transition probability between different magnon bands, which is associated with the nonadiabatic Landau-Zener tunneling [27–34]. In contrast to the charge or spin current carried by electrons, the magnon spin current driven by electric field is drastically different in the two cases. For the magnon spin current in collinear ferromagnet (FM), the magnitude is sourced in the electric field component that perpendicular to the magnetization direction. On the other hand, a nonzero magnon spin current requires the time-varying driving electric field, while such constraint is absence for the charge current. Finally we propose 1D SSH FM as possible candidates to realize the electric field driven magnon spin current. Our results suggest that collinear FM can serve as effective spin current generators and provide a promising platform to explore novel magnonic effects.

II. A GENERAL DESCRIPTION

We consider the magnon transport driven by time-dependent electric field and calculate the real-time magnon spin current. In the presence of electric field, a moving magnetic dipole moment (magnon) associated

* zgzhu@ucas.ac.cn

† gsu@ucas.ac.cn

with the spin along z acquires a geometric phase called the Aharonov-Casher (AC) phase [26]:

$$\theta_{ij} = \frac{g\mu_B}{\hbar c^2}\int_{\boldsymbol{r}_i}^{\boldsymbol{r}_j} (\boldsymbol{E}(t) \times \hat{\boldsymbol{e}}_z) \cdot d\boldsymbol{r}. \tag{1}$$

Where we suppose that the magnetization direction is along z-direction, hence the magnetic moment of a magnon is $\boldsymbol{\mu} = -g\mu_B\hat{\boldsymbol{e}}_z$, with μ_B the Bohr magneton and g the Landé factor. It has been elucidated that the AC phase is a special case of Berry phase [39], in parallel to the well-known AB phase. Starting from a spin Hamiltonian, it has been shown that the electric field is accounted for by introducing the canonical momentum incorporated with an effective vector potential [40–42]. Here, we show that for collinear ferromagnet the single-particle Hamiltonian of magnon takes the form of minimal coupling (See Appendix. A for details):

$$\mathcal{H}_A(\boldsymbol{k}, t) = \mathcal{H}_0(\boldsymbol{k} - \frac{g\mu_B}{\hbar c}\boldsymbol{A}_{\text{eff}}(t)), \tag{2}$$

where the effective vector potential is defined by

$$\boldsymbol{A}_{\text{eff}}(t) = \frac{1}{c}\boldsymbol{E}(t) \times \hat{\boldsymbol{e}}_z. \tag{3}$$

Alternatively, the perturbed Hamiltonian Eq. (2) can be written in form of an effective dipole interaction via an unitary transformation (for details see Appendix.B)

$$\mathcal{H}_E(\boldsymbol{k}, t) = \mathcal{H}_0(\boldsymbol{k}) + \frac{g\mu_B}{c}\boldsymbol{\mathcal{E}}(t) \cdot \boldsymbol{r}, \tag{4}$$

where $\mathcal{H}_0$ is the single-magnon Hamiltonian in crystal momentum space. In Eq. (4) we introduce the effective electric field via effective vector potential

$$\boldsymbol{\mathcal{E}}(t) \equiv -\frac{\partial \boldsymbol{A}_{\text{eff}}(t)}{\partial t}, \tag{5}$$

which is in analogy with the electron dipole interaction using magnetic vector potential. According to Eq. (3) and Eq. (5), it is seen that the electric field $\boldsymbol{E}$ has to be time-varying, otherwise the effective electric field $\boldsymbol{\mathcal{E}}$ as well as the effective dipole interaction are zero when dc electric field is applied. Noting that the perturbation Hamiltonian Eq. (4) of magnons presents a formal duality to that of electron system with dipole interaction perturbation. However, the effective vector potential $\boldsymbol{A}_{\text{eff}}$ does not have a gauge freedom, in contrast to the magnetic vector potential. The analogy between the electric field perturbed Hamiltonian of magnons and that of electrons are shown in Table. I.

We recall that the magnon eigenstates in an unperturbed crystal is $\mathcal{H}_0 |u_n, \boldsymbol{k}(t)\rangle = \varepsilon_{n,\boldsymbol{k}} |u_n, \boldsymbol{k}\rangle$. When consider the electric field perturbation and make use of the dipole Hamiltonian Eq. (4), the single-particle time-dependent Schördinger equation is written as

$$i\hbar\partial_t |\Psi_m, \boldsymbol{k}_0(t)\rangle = \mathcal{H}_E(\boldsymbol{k}, t) |\Psi_m, \boldsymbol{k}_0(t)\rangle, \tag{6}$$

TABLE I. List of the analogy between then dipole interaction of magnons via Aharonov-Casher phase and that of electrons via Aharonov-Bohm phase.

	electron	magnon
"Charge"	e	$g\mu_B/c$
Vector potential	$\boldsymbol{A}$	$\boldsymbol{A}_{\text{eff}} = \frac{1}{c}\boldsymbol{E} \times \hat{\boldsymbol{e}}_z$
Gauge freedom of $\boldsymbol{A}$ and $\boldsymbol{A}_{\text{eff}}$	✓	×
"Electric field"	$\boldsymbol{E} = -\frac{\partial \boldsymbol{A}}{\partial t}$	$\boldsymbol{\mathcal{E}} = -\frac{1}{c}\frac{\partial \boldsymbol{E}}{\partial t} \times \hat{\boldsymbol{e}}_z$
Time constraint on $\boldsymbol{E}$	×	✓

where the general magnon instantaneous state in Bloch representation is given by

$$|\Psi_m, \boldsymbol{k}_0(t)\rangle = \sum_n C_{mn\boldsymbol{k}_0}(t)e^{i\gamma_{n\boldsymbol{k}_0}(t)} |u_n, \boldsymbol{k}(t)\rangle, \tag{7}$$

with $\boldsymbol{k}_0 = \boldsymbol{k}(t = 0)$, and the subscript m in $|\Psi_{m\boldsymbol{k}_0}(t)\rangle$ denotes the initial condition $C_{mm\boldsymbol{k}_0}(t_0) = 1$. The phase γ includes a dynamical and a geometric phase, which is given by

$$\gamma_{n\boldsymbol{k}_0} = \int_0^t dt_1 \left[\varepsilon_n(\boldsymbol{k}_0(t_1)) + \frac{g\mu_B}{c}\boldsymbol{\mathcal{E}}(t_1) \cdot \boldsymbol{\mathcal{A}}_{nn}(\boldsymbol{k}_0(t_1))\right]/\hbar \tag{8}$$

in which $\boldsymbol{\mathcal{A}}_{nn} = i\langle u_n, \boldsymbol{k}(t)| \nabla_{\boldsymbol{k}} |u_n, \boldsymbol{k}(t)\rangle$ denotes the intraband Berry connection. Recently the nonlinear response has been investigated at great length, it has been discovered that the geometric nature of the wave functions plays a significant role in the Landau-Zener tunneling [35–37]. In band insulators with PT symmetry, it has been revealed that the spin current carried by electrons is generated, which is raised by Landau-Zener tunneling in strong dc electric field [38]. Inspired by the progress in electron systems, we generate the tunnelling concept to magnon transport. By inserting Eq. (7) and Eq. (8) into he time-dependent Schördinger equation Eq. (6) and making use of the initial conditions, we obtain (see Appendix. C)

$$\begin{aligned} i\partial_t C_{ln\boldsymbol{k}_0}(t) =& \frac{g\mu_B}{\hbar c}\sum_{m\neq n}\mathcal{E}^\alpha|\mathcal{A}^\alpha_{nm}(\boldsymbol{k}_0(t))|e^{i\arg\mathcal{A}^\alpha_{nm}(\boldsymbol{k}_0(t_0))} \\ &\times e^{i\int_{t_0}^{t_1} dt_2\Delta_{mn}(\boldsymbol{k}_0(t_2))/\hbar}C_{lm\boldsymbol{k}_0}(t), \end{aligned} \tag{9}$$

where $\mathcal{A}^\alpha_{nm}$ is the inter-band Berry connection and $\Delta^\alpha_{nm}(\boldsymbol{k})$ is introduced as $\Delta^\alpha_{nm}(\boldsymbol{k}) = \varepsilon_n(\boldsymbol{k}) - \varepsilon_m(\boldsymbol{k}) + \frac{g\mu_B}{c}\mathcal{E}^\alpha(t)R^{\alpha\beta}_{nm}(\boldsymbol{k})$, $R^{\alpha\beta}_{nm}(\boldsymbol{k}) = \mathcal{A}^\beta_{nn}(\boldsymbol{k}) - \mathcal{A}^\beta_{mm}(\boldsymbol{k}) - \partial_{k_\beta}\arg\mathcal{A}^\alpha_{nm}(\boldsymbol{k})$ is the magnon shift vector [25, 43], which characterizes the spin polarization difference between two magnon bands m and n, which shares a similar expression with the electronic shift vector in semiconductors [36, 44–46]. Making use of the canonical equations

$\hbar\dot{\boldsymbol{k}} = -\partial\mathcal{H}_E/\partial\boldsymbol{r}$, the acceleration of wave vector is given by

$$\hbar\dot{\boldsymbol{k}} = -\frac{g\mu_B}{c}\boldsymbol{\mathcal{E}}(t). \tag{10}$$

By integrating Eq. (9) from t_0 to t, we have

$$\begin{pmatrix} C_{nm\boldsymbol{k}_0(t)}e^{-i\arg\mathcal{A}^\alpha_{mn}(\boldsymbol{k}_0)} \\ C_{nn\boldsymbol{k}_0(t)}e^{i\arg\mathcal{A}^\alpha_{mn}(\boldsymbol{k}_0)} \end{pmatrix} = \exp\left[-i\int_{t_0}^{t} dt_1 \frac{g\mu_B}{\hbar c}\mathcal{E}^\alpha(t_1)|\mathcal{A}^\alpha_{mn}(\boldsymbol{k}_0(t_1))| \begin{pmatrix} 0 & W(t_1) \\ W^*(t_1) & 0 \end{pmatrix}\right]\begin{pmatrix} 0 \\ 1 \end{pmatrix}. \tag{11}$$

where $W(t_1) = \exp\left[i\int_{t_0}^{t_1} dt_2\Delta_{mn}(\boldsymbol{k}_0(t_2))/\hbar\right]$. In deriving Eq. (11) we used Eq. (10) and the initial conditions $C_{mm\boldsymbol{k}_0}(t_0) = 1$. The probability of magnons with momentum $\boldsymbol{k}_0$ tunnelling from n-band to m-band is defined as

$$P_{nm\boldsymbol{k}_0}(t) = |\langle m, \boldsymbol{k}_0(t)\,|\Psi_n, \boldsymbol{k}_0(t)\rangle\,|^2 = |C_{nm\boldsymbol{k}_0}(t)|^2. \tag{12}$$

Noting that $P_{nm\boldsymbol{k}_0}(t)$ is gauge-invariant because of the gauge-invariance of $\mathcal{A}^\alpha_{mn}$ and $R^{\alpha\beta}_{nm}$. The of the z-direction polarized magnon spin current is given as an expectation value of the magnon spin current operator for all magnons in BZ, which is given by

$$\boldsymbol{J}^s_z = \sum_{\boldsymbol{k}_0\in BZ}\sum_n \hbar f_{n,\boldsymbol{k}_0}\langle\Psi_n, \boldsymbol{k}_0(t)|\,\hat{\boldsymbol{J}}^s_{\boldsymbol{k}_0,z}(t)\,|\Psi_n, \boldsymbol{k}_0(t)\rangle\,, \tag{13}$$

where $f_{n,\boldsymbol{k}_0} = 1/(e^{-\beta\varepsilon_n(\boldsymbol{k}_0)} - 1)$ is the Bose-Einstein distribution with the chemical potential set to zero (since the magnon number is not conservative), $\hat{\boldsymbol{J}}^s_{\boldsymbol{k},z}$ is the z-direction polarized magnon spin current operator. By use of the periodic boundary conditions, Eq. (13) can be alternatively written as (for derivations see Appendix. D)

$$\boldsymbol{J}^s_z = -\sum_{n,m}\int\frac{d\boldsymbol{k}_0}{2\pi} f_{n,\boldsymbol{k}_0}\nabla_{\boldsymbol{k}}\left[\varepsilon_{nm}(\boldsymbol{k})P_{mn}(\boldsymbol{k})\right]|_{\boldsymbol{k}=\boldsymbol{k}_0(t)}. \tag{14}$$

where ε_{nm} is introduced as $\varepsilon_{nm} = \varepsilon_n - \varepsilon_m$. In Eq. (14) we use the identity $C_{mn} = C^*_{nm}$.

III. ELECTRIC FIELD DRIVEN MAGNON SPIN CURRENT IN 1D SPIN CHAIN

A. Model Hamiltonian and formulation

To elucidate the emergence of the electric-field-driven magnon spin current, we apply our theory to 1D ferromagnetic (FM) SSH model [47]. The spin Hamiltonian of the 1D spin chain is written as

$$H = -J_1\sum_{i=1}^{N}\boldsymbol{S}_{i,A}\cdot\boldsymbol{S}_{i,B} - J_1\sum_{i=1}^{N-1}\boldsymbol{S}_{i,B}\cdot\boldsymbol{S}_{i+1,A} - \sum_i K_i(S^z_i)^2, \tag{15}$$

where J_1 and J_2 represent the exchange interaction in the unit cell (intracellular) and between the two unit cells (intercellular), respectively. The last term is the easy-axial anisotropy term for the quantization z-axis, where K_i is the axial anisotropy energy. From an inspection of the cross product form of Eq. (1), for nonzero magnon spin current, a requirement is that the electric field should have nonzero component perpendicular to the magnetization direction. Another requirement from the direct product form in Eq. (4) is that the electric field should have nonzero component perpendicular to the 1D spin chain. As shown in Fig. 1, where the 1D spin chain and the generated magnon spin current is on x-axis with the magnetization along z-axis, and the time-varying electric-field is applied on y-direction.

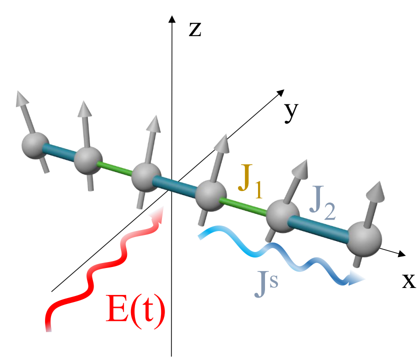

FIG. 1. Magnon spin current generated by ac electric field for a 1D FM SSH model. The ac electric field with red arrow is perpendicular to the spin chain and the magnetization axis.

The linear Holstein–Primakoff (HP) transformation gives the magnon Hamiltonian with bosonic generation (annihilation) operator (for A sublattice, $a^\dagger_A$ (a_A); for B

sublattice, $a_B^\dagger$ (a_B)), which is expressed as

$$
\begin{aligned}
H =&(J_1+J_2+K)S\sum_{i=1}^{N}(a_{i,A}^\dagger a_{i,A}+a_{i,B}^\dagger a_{i,B})\\
&-J_1S\sum_{i=1}^{N}(a_{i,A}^\dagger a_{i,B}+a_{i,B}^\dagger a_{i,A})\\
&-J_2S\sum_{i=1}^{N-1}(a_{i,A}^\dagger a_{i+1,B}+a_{i+1,B}^\dagger a_{i,A}).
\end{aligned}
\tag{16}
$$

In k-space it is given as $H=\Phi_k^\dagger\mathcal{H}_k\Phi_k$, where $\Phi^\dagger=(a_{k,A}^\dagger,a_{k,B}^\dagger)$, and the single-particle Hamiltonian is

$$
\mathcal{H}(k)=\varepsilon_0 I+\mathrm{Re[f(k)]}\sigma_\mathrm{x}+\mathrm{Im[f(k)]}\sigma_\mathrm{y},\tag{17}
$$

in which $\varepsilon_0=(J_1+J_2+K)S$, $f(k)=-J_1S-J_2Se^{-ika}$ with a being the lattice constant, and I, σ_x, σ_y being the unit and Pauli matrix. The classical ground state is identified by treating the quantum mechanical spins as classical vectors and minimizing the classical ground-state energy. According to Eq. (14), for 1D two bands system, the expression of magnon spin current reduces to

$$
J_z^s=\int\frac{dk_0}{2\pi}f_{+-,k_0}\partial_k\left[\varepsilon_{+-}(k)P_{-+}(k)\right]|_{k=k_0(t)},\tag{18}
$$

where we introduce $f_{+-}=f_- - f_+$.

Now we illustrate a symmetry consideration. The 1D FM SSH model preserves the spacial inversion symmetry, which is defined as $\mathcal{P}\mathcal{H}(k)\mathcal{P}^{-1}=\mathcal{H}(-k)$,, with the inversion operation $\mathcal{P}=\sigma_x$. Under the spacial inversion, the Berry connections satisfy $\mathcal{A}_{mn}^\alpha(k)=-\mathcal{A}_{mn}^\alpha(-k)$, and the shift vector transforms as $R_{mn}^{\alpha\beta}(k)=-R_{mn}^{\alpha\beta}(-k)$. However, the time-reversal symmetry (TRS) $\mathcal{T}$ is not preserved. Instead, it respects to the effective TRS $\mathcal{T}'$, which is a combination of the TRS $\mathcal{T}$ and a spin rotation by π about the direction perpendicular to the quantization axis, i.e., $\mathcal{T}'\mathcal{H}(k)(\mathcal{T}')^{-1}=\mathcal{H}(-k)$,which gives a constraint on the Berry connections $\mathcal{A}_{mn}^\alpha(k)=\mathcal{A}_{nm}^\alpha(-k)$, and the shift vector satisfies $R_{mn}^{\alpha\beta}(k)=R_{mn}^{\alpha\beta}(-k)$. Combining the inversion symmetry and the effective TRS, it yields $R_{mn}^{\alpha\beta}(k)=0$. As we will discuss below, nontrivial effect is associated with finite $R_{mn}^{\alpha\beta}$ owing to broken inversion symmetry.

B. Electric field driven magnon spin current

For a 1D infinite system, the topological properties in the momentum k-space are often described by the Zak phase $\varphi_{\mathrm{Zak}}(n)=\int_{\mathrm{BZ}}\mathcal{A}_{nn}dk$. For the magnon Hamiltonian Eq. (17), a topological phase transition occurs at a critical ratio $J_1/J_2=1$ accompanied by energy gap closing [47], which distinguishes the topological trivial phase ($J_1/J_2>1$) and topological nontrivial phase ($J_1/J_2<1$).

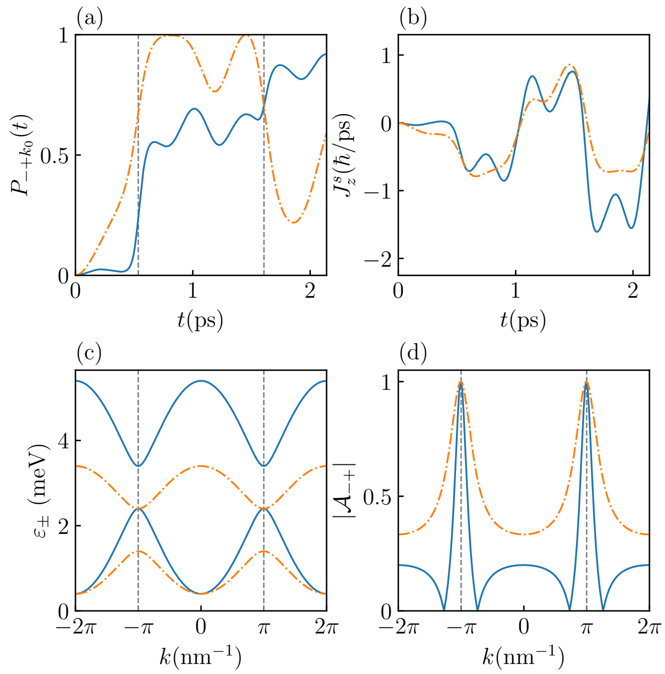

FIG. 2. Magnon Landau-Zener tunneling in 1D FM SSH model with both effective TRS and inversion symmetry. The solid (dashed-dot) line corresponds to the ratio $J_1/J_2=1.5$ ($J_1/J_2=0.5$) which is topological trivial (non-trivial). (a) Tunneling probability P_{-+k_0} for wave vector $k_0=-2\pi$ as a function of time, for which the electric field is switched on at $t=0$. (b) The magnon spin current. (c) The band dispersion. (d) The absolute value of the interband Berry connection $\mathcal{A}_{-+}$. The dashed vertical lines in (c) and (d) show the wave vector k where the band gap is locally minimum, for that in (a) is the corresponding $t(k)$. Parameters are $J_2=1$meV, $K=0.4$meV, $k_BT=1$meV, $t_c=10^{-9}$ps, $a=1$nm, $E_0=1.5\times10^4$V/nm.

For simplicity, we consider the time-dependent electric field which linearly increase with time, yielding a constant effective field $\mathcal{E}$. The time-dependent electric field is written as $E(t)=E_0t/t_c$, with a characteristic time t_0, and we have $\mathcal{E}=E_0/ct_c$. The time evolution of $P_{-+k_0}(t)$ is depicted in Fig. 2(a). It is seen the tunnelling probability $P_{-+k_0}(t)$ for both of the topological nontrivial phase $J_1/J_2=0.5$ and the trivial phase $J_1/J_2=1.5$ show sharp change at the time point of t_{g_1}, t_{g_2} (dashed lines) that corresponding to the locations of gap $k=k_0(t_{g_1})=-\pi$, $k=k_0(t_{g_2})=\pi$ (as displayed by Fig. 2(c)), as a typical manifestation of the Landau-zener tunnelling. The derivative of $P_{-+k_0}(t)$ is written as $\dot{P}_{-+k_0}(t)=2C_{nmk_0}(t)\dot{C}_{nmk_0}(t)$. Combining to Eq. (9), it is found that $\dot{P}_{-+k_0}(t)$ scales with $|\mathcal{A}_{-+}(k)|$. We show $|\mathcal{A}_{-+}(k)|$ for the topological trivial and nontrivial phase in Fig. 2(d). It is seen that $|\mathcal{A}_{-+}(k)|$ vanishes around the location of gap for the topological phase, this explains the a pair of peaks of $P_{-+k_0}(t)$ around t_g for the topological trivial case in Fig. 2(a). We depict the evolution of the magnon spin current J_z^s in Fig. 2(b). It is seen that J_z^s for both of the topological trivial and nontrivial case show an oscillating behavior. This is because that the Hamiltonian $H(k(t))$ is time-periodic with period $T = 2\pi\hbar c/(g\mu_B\mathcal{E}a)$, which is in analogy with the Bloch oscillation of the electrons [38].

C. Nonreciprocal magnon transport

Noting that the magnon spin current calculated above is reciprocal owing to the inversion symmetry. When the inversion symmetry is broken, the nonreciprocal transport behaviour is expected. The nonreciprocal phenomena of electron transport in noncentrosymmetric system have been extensively studied [48–50], recently it has been shown that the electron transport nonreciprocity is associated with Landau-Zener tunnelling [36]. In a noncentrosymmetric magnetic-ordered state, such nonreciprocity should be also expected for magnons [51–53].

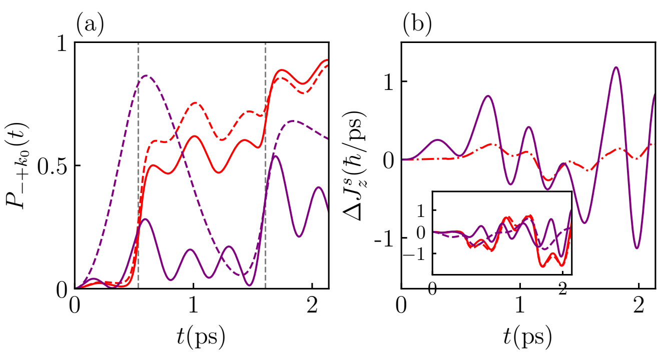

FIG. 3. Magnon Landau-Zener tunneling in 1D FM SSH model with broken inversion symmetry. (a) Tunneling probability P_{-+k_0} for wave vector $k_0 = -2\pi$ as a function of time, for which the electric field is switched on at $t = 0$. The solid (dashed-dot) line corresponds to the ratio $J_1/J_2 = 1.5$ ($J_1/J_2 = 0.5$) which is topological trivial (non-trivial), the red (purple) line corresponds to $E_0 = 1.5 \times 10^4$ V/nm ($E_0 = -1.5 \times 10^4$ V/nm). (b) The nonreciprocal magnon spin current ΔJ_z^s as a function of time. The inset shows the magnon spin current $J_z^s(+E)$ and $J_z^s(-E)$ with forward and reverse electric field applied, respectively. The on-site energy $m = 0.1$ meV, other parameters are same as that in Fig. 2.

Now we investigate the possible magnon spin current nonreciprocity in the 1D FM SSH model. We add an onsite energy for the A and B sites of m and $-m$ respectively, it would introduce a term $H_m = m\sum_{i=1}^{N}(a_i^\dagger a_i - b_i^\dagger b_i)$, which breaks the inversion symmetry. Consequently, the single-particle Hamiltonian would add a σ_z term, which is written as $\mathcal{H}_m = m\sigma_z$. In Fig. 3(a) we depict the tunneling probabilities of the topological trivial and nontrivial phase for wave vector $k_0 = -2\pi$ as a function of time. It is seen that the both of tunneling probability for the topological trivial and nontrivial phase split owing to the broken inversion symmetry. Consequently, we see the split of $J_z^s(+E)$ and $J_z^s(-E)$, as shown in the inset of Fig. 3(b), resulting to the nonreciprocity of magnon transport, which is defined by the nonreciprocal magnon spin current $\Delta J_z^s = J_z^s(+E) - J_z^s(-E)$. The nonreciprocity shows up for both the topological trivial and nontrivial phase once the electric field is applied, as shown in Fig. 3(b). As mentioned, breaking of inversion symmetry leads to finite shift vector $R_{mn}(k)$, which yields the nonreciprocity.

IV. CONCLUDING REMARKS

In summary, we investigated the magnon spin current driven by time-varying electric field. The magnon spin current arises due to the effective dipole interaction between magnon and electric field. By solving time-dependent Schördinger equation the magnon response is considered nonperturbatively. There are two distinct restrictions on the electric field to obtain finite magnon spin current: the first is that the direction of electric field should be perpendicular to the magnetization axis, the second is the electric field need to be time-varying. We applied our theory to 1D ferromagnetic SSH model with linearly increasing electric field applied, and observed a time-varying magnon spin current, as expected. Different topological phases are characterized by inter-band Berry connection and manifest in Zener tunnelling processes. By adding a on-site energy, it is found that the nonreciprocal magnon transport arises due finite magnon shift vector with broken inversion symmetry.

Noting that in this study we restricted the discussion within collinear ferromagnet. Notably, other magnetic states such as antiferromagnetic, spiral, chiral states potentially have different advantages such as faster response [54], it is worthy pointing out that our theory can be directly generalized to more complicated magnetic states, which deserves a further study.

ACKNOWLEDGMENTS

This work is supported in part by National Key R&D Program of China (Grant No. No. 2022YFA1402802), NSFC (Grants No. 11974348 and No. 11834014), the Strategic Priority Research Program of CAS (Grants No. XDB28000000, and No. XDB33000000), the Training Program of Major Research plan of the National Natural Science Foundation of China (Grant No. 92165105), and CAS Project for Young Scientists in Basic Research Grant No. YSBR-057.

Appendix A: Magnon Hamiltonian and electric-field perturbation

1. Linear spin-wave theory

Here we rewrite the general two-body spin interaction Hamiltonian,

$$H = \frac{1}{2}\sum_{i,j}^{L}\sum_{n,m}^{N}\sum_{\alpha\beta} S_{i,n}^{\alpha} H_{nm}^{\alpha\beta}(i-j) S_{j,m}^{\beta}, \tag{A1}$$

By setting a global (reference) coordinates $(\hat{\boldsymbol{x}}, \hat{\boldsymbol{y}}, \hat{\boldsymbol{z}})$, the local coordinates (spherical coordinates) of each spin relate the global coordinate through

$$\boldsymbol{S}_{i,n} = R_n(\theta_i, \phi_i)\boldsymbol{S}_0. \tag{A2}$$

The classical ground state is identified by treating the quantum mechanical spins operators as classical vectors and minimizing the classical ground-state energy. The magnons are the usual low-energy excitation in ordered magnets, which is considered via the Holstein-Primakoff transformation in local coordinates [55, 56]

$$\begin{aligned} &S_{i,n}^{\theta} = \sqrt{\frac{S}{2}}(a_{i,n} + a_{i,n}^{\dagger}), \quad S_{i,n}^{\phi} = -i\sqrt{\frac{S}{2}}(a_{i,n} - a_{i,n}^{\dagger}), \\ &S_{i,n}^{r} = S - a_{i,n}^{\dagger} a_{i,n}. \end{aligned} \tag{A3}$$

and we obtain

$$\boldsymbol{S}_{i,n}^{\alpha} = \sqrt{\frac{S}{2}}\hat{\boldsymbol{u}}_n a_{i,n} + \sqrt{\frac{S}{2}}\hat{\boldsymbol{u}}_n^{*} a_{i,n}^{\dagger} + \hat{\boldsymbol{z}}_n(S - a_{i,n}^{\dagger}a_{i,n}), \tag{A4}$$

In which $\alpha = x, y, z$, the coefficients $\hat{\boldsymbol{u}}_n$ and $\hat{\boldsymbol{z}}_n$ are related to the relative rotation between the global and local coordinates, that are explicitly written as

$$\begin{aligned} \begin{pmatrix} u_n^x \\ u_n^y \\ u_n^z \end{pmatrix} &= \begin{pmatrix} \cos\theta_n\cos\phi_n + i\sin\phi_n \\ \cos\theta_n\cos\phi_n - i\sin\phi_n \\ -\sin\theta_n \end{pmatrix}, \\ \begin{pmatrix} z_n^x \\ z_n^y \\ z_n^z \end{pmatrix} &= \begin{pmatrix} \sin\theta_n\cos\phi_n \\ \sin\theta_n\sin\phi_n \\ \cos\theta_n \end{pmatrix}. \end{aligned} \tag{A5}$$

Expanding the coupling interaction, we obtain

$$\begin{aligned} S_{i,n}^{\alpha} S_{j,m}^{\beta} =& \frac{1}{2} u_n^{\alpha *} a_{i,n}^{\dagger}(u_m^{\beta} a_{j,m} + u_m^{\beta *} a_{j,m}^{\dagger}) \\ &+ \frac{1}{2} u_n^{\alpha} a_{i,n}(u_m^{\beta *} a_{j,m}^{\dagger} + u_m^{\beta} a_{j,m}) \\ &- z_n^{\alpha} z_m^{\beta}(a_{i,n}^{\dagger} a_{i,n} + a_{j,m}^{\dagger} a_{j,m}). \end{aligned} \tag{A6}$$

By inserting Eq. (A6) into Eq. (A1), we have

$$\begin{aligned} H =& \sum_{i,j,n,m} A_{nm}(i-j) a_{i,n}^{\dagger} a_{j,m} \\ &+ \frac{1}{2}\sum_{i,j,n,m}\left[B_{nm}(i-j) a_{i,n}^{\dagger} a_{j,m}^{\dagger} + \text{h.c.}\right] \\ &+ 2\sum_{i,n,m} C_{nm} a_{i,n}^{\dagger} a_{i,n}. \end{aligned} \tag{A7}$$

In which

$$\begin{aligned} A_{nm}(i-j) &= \frac{\sqrt{S_n S_m}}{2}\sum_{\alpha\beta} u_n^{\alpha *} H_{nm}^{\alpha\beta}(i-j) u_m^{\beta}, \\ B_{nm}(i-j) &= \frac{\sqrt{S_n S_m}}{2}\sum_{\alpha\beta} u_n^{\alpha *} H_{nm}^{\alpha\beta}(i-j) u_m^{\beta *}, \\ C_{nm} &= \delta_{nm} S_l \sum_{\alpha\beta} z_n^{\alpha} \sum_{j}\sum_{l} H_{nm}^{\alpha\beta}(i-j) z_l^{\beta}. \end{aligned} \tag{A8}$$

By transforming Eq. (A6) to the reciprocal space, there is

$$a_{i,n} = (1/\sqrt{L})\sum_{\boldsymbol{k}} \exp\left[i\boldsymbol{k}\cdot(\boldsymbol{r}_i + \boldsymbol{t}_n)\right] a_{\boldsymbol{k},n}, \tag{A9}$$

where $\boldsymbol{r}_i$ is the position of the ith unit cell and $\boldsymbol{t}_m$ is the relative vector of the mth sublattice. We have $H = \frac{1}{2}\sum_{\boldsymbol{k}} \Psi_{\boldsymbol{k}}^{\dagger}\mathcal{H}(\boldsymbol{k})\Psi_{\boldsymbol{k}}$, where

$$\mathcal{H}(\boldsymbol{k}) = \begin{pmatrix} A(\boldsymbol{k}) - C & B(\boldsymbol{k}) \\ B^{\dagger}(\boldsymbol{k}) & A^{T}(-\boldsymbol{k}) - C \end{pmatrix} \tag{A10}$$

is a 2N×2N bosonic Bogoliubov-de Gennes (BdG) Hamiltonian with the vector boson operator where $\Psi_{\boldsymbol{k}}^{\dagger} = (a_{\boldsymbol{k},1}^{\dagger}, \cdots, a_{\boldsymbol{k},N}^{\dagger}, a_{-\boldsymbol{k},1}, \cdots, a_{-\boldsymbol{k},N})$, and the $N \times N$ block matrix is given by

$$\begin{aligned} A_{mn}(\boldsymbol{k}) &= \sum_{\alpha,\beta} u_n^{\alpha *}\left[\sum_{\boldsymbol{d}} e^{-i\boldsymbol{k}\cdot\boldsymbol{d}} H_{nm}^{\alpha\beta}(\boldsymbol{d})\right] u_m^{\beta}, \\ B_{mn}(\boldsymbol{k}) &= \sum_{\alpha,\beta} u_n^{\alpha *}\left[\sum_{\boldsymbol{d}} e^{-i\boldsymbol{k}\cdot\boldsymbol{d}} H_{nm}^{\alpha\beta}(\boldsymbol{d})\right] u_m^{\beta *}, \\ C_{mn} &= \delta_{mn}\sum_{\alpha,\beta}\sum_{l} z_n^{\alpha *}\left[\sum_{\boldsymbol{d}} H_{nl}^{\alpha\beta}(\boldsymbol{d})\right] z_l^{\beta}. \end{aligned} \tag{A11}$$

Where $\boldsymbol{d} = (\boldsymbol{r}_i + \boldsymbol{t}_n) - (\boldsymbol{r}_j - \boldsymbol{t}_m)$ is the difference vector between the mth and the nth spin. In deriving Eq. (A11) the relation

$$\sum_{\boldsymbol{k}}\sum_{n,m} A_{nm}(\boldsymbol{k}) a_{\boldsymbol{k},n}^{\dagger} a_{\boldsymbol{k},m} = \sum_{\boldsymbol{k}}\sum_{n,m} A_{nm}^{T}(-\boldsymbol{k}) a_{-\boldsymbol{k},n} a_{-\boldsymbol{k},m}^{\dagger} \tag{A12}$$

is used. For collinear ferromagnets, the Hamiltonian Eq. (A10) is block diagonal with identical block which can be reduced to $H = \sum_{\boldsymbol{k}} \Psi_{\boldsymbol{k}}\mathcal{H}_{\boldsymbol{k}}\Psi_{\boldsymbol{k}}$ with $\mathcal{H}_{\boldsymbol{k}} = (A_{\boldsymbol{k}} - C)$ and $\Psi_{\boldsymbol{k}}^{\dagger} = (a_{\boldsymbol{k},1}^{\dagger}, \cdots, a_{\boldsymbol{k},N}^{\dagger})$.

In general the bosonic Hamiltonian Eq. (A10) does not conserve the particle number, for example, the ferromagnets with elliptical magnons (where an anisotropy deforms the formerly circular precession) or in non-ferromagnets. And the Hamiltonian is diagonalized with the Bogoliubov transformation

$$U_{\boldsymbol{k}}^{\dagger}\mathcal{H}_{\boldsymbol{k}} U_{\boldsymbol{k}} = \mathcal{E}_{\boldsymbol{k}}, \tag{A13}$$

which satisfies $U_{\boldsymbol{k}}\Sigma_z U_{\boldsymbol{k}}^{\dagger} = \Sigma_z$, where the diagonal matrix $\Sigma_z = \text{diag}(1, 1, \cdots, -1, -1, \cdots)$ with N positive ones and

N minus ones along the diagonal. The vector boson operator transforms as $\Psi_{\boldsymbol{k}} = U_{\boldsymbol{k}}\Phi_{\boldsymbol{k}}$. The mth column vector encoded in the matrix $U_{\boldsymbol{k}}$ stands for the (periodic part of) Bloch wave function for the mth magnon band [57]. Noting that $\Phi_{\boldsymbol{k}}$ does not satisfy the commutation relation of Bosons. Instead it satisfies

$$[\Phi_{\boldsymbol{k}}, \Phi^\dagger_{\boldsymbol{k}'}] = \Sigma_z \delta_{\boldsymbol{k},\boldsymbol{k}'}. \tag{A14}$$

The equilibrium density matrix in band space is given as

$$\rho^{(0)}_{\boldsymbol{k}m}(t) \equiv \langle (\Phi^\dagger_{\boldsymbol{k}})_m(t)(\Phi_{\boldsymbol{k}})_m(t)\rangle_0. \tag{A15}$$

Where the subscript "0" denotes the equilibrium state, and $(\Phi^\dagger_{\boldsymbol{k}})_m$ is the mth element of the vector $\Phi^\dagger_{\boldsymbol{k}}$. For later convenience, we write $(\Phi^\dagger_{\boldsymbol{k}})_m$ as $\Phi^\dagger_{\boldsymbol{k}m}$. By using of Eq. (A14), one obtains

$$\rho_{\boldsymbol{k}m} = \begin{cases} g(\mathcal{E}_{\boldsymbol{k}m}), & [\Phi_{\boldsymbol{k}m}, \Phi^\dagger_{\boldsymbol{k}m}] = 1 \\ -g(-\mathcal{E}_{\boldsymbol{k}m}), & [\Phi_{\boldsymbol{k}m}, \Phi^\dagger_{\boldsymbol{k}m}] = -1, \end{cases} \tag{A16}$$

where $g(\mathcal{E}_{\boldsymbol{k}m})$ is the Bose-Einstein distribution $g(\mathcal{E}_{\boldsymbol{k}m}) = 1/(e^{\beta\mathcal{E}_{\boldsymbol{k}m}} - 1)$. It is convenient to introduce the matrix $\varepsilon_{\boldsymbol{k}}$ [25]:

$$\varepsilon_{\boldsymbol{k}} = \Sigma_z \mathcal{E}_{\boldsymbol{k}} = U^{-1}_{\boldsymbol{k}}\Sigma_z\mathcal{H}_{\boldsymbol{k}}U_{\boldsymbol{k}}, \tag{A17}$$

and the density matrix is simplified as $\rho_{\boldsymbol{k}m} = \Sigma_{z,mm}g(\varepsilon_{\boldsymbol{k}m})$. For general operator, with the Bogolyubov's representation, it transforms

$$\hat{O} = \sum_{\boldsymbol{k}} \Psi^\dagger_{\boldsymbol{k}}\mathcal{O}_{\boldsymbol{k}}\Psi_{\boldsymbol{k}} = \sum_{\boldsymbol{k}} \Phi^\dagger_{\boldsymbol{k}}\Sigma_z\tilde{\mathcal{O}}_{\boldsymbol{k}}\Phi_{\boldsymbol{k}} \tag{A18}$$

with the definition $\tilde{\mathcal{O}}_{\boldsymbol{k}} = U^{-1}_{\boldsymbol{k}}\Sigma_z\mathcal{O}U_{\boldsymbol{k}}$.

2. Perturbation of electric field in form of minimal coupling for collinear ferromagnet and antiferromagnet

Now we consider the AC effect. In Eq. (A6) the first two terms describe the magnon hopping. In the presence of electric field, the magnon acquires a phase while travelling between the mth and the nth spin on the ith and jth site, which is given by

$$\theta_{in,jm} = -\frac{g\mu_B}{\hbar c^2}\int_{\boldsymbol{r}_{i,n}}^{\boldsymbol{r}_{j,m}} (\boldsymbol{E}(t) \times \hat{\boldsymbol{e}}_n)\cdot d\boldsymbol{r}, \tag{A19}$$

The coupling interaction is modified as

$$\begin{aligned} S^\alpha_{i,n}S^\beta_{j,m} =& \frac{1}{2}U^{\alpha*}_n a^\dagger_{i,n}(U^\beta_m a_{j,m} + U^{\beta*}_m a^\dagger_{j,m})e^{i\theta_{in,jm}} \\ &+ \frac{1}{2}U^\alpha_n a_{i,n}(U^{\beta*}_m a^\dagger_{j,m} + U^\beta_m a_{j,m})e^{-i\theta_{in,jm}} \\ &- V^\alpha_n V^\beta_m(a^\dagger_{i,n}a_{i,n} + a^\dagger_{j,m}a_{j,m}). \end{aligned} \tag{A20}$$

Suppose that the scale of the spacial variance of $\boldsymbol{E}$ is much larger than lattice constant and introducing the effective vector potential $\boldsymbol{A}_{\text{eff},n} = \frac{1}{c}\boldsymbol{E}\times\hat{\boldsymbol{e}}_n$, one obtains

$$\theta_{in,jm} = \frac{g\mu_B}{\hbar c}\boldsymbol{A}_{\text{eff},n}\cdot\boldsymbol{d}, \tag{A21}$$

Following the same procedure, we have

$$\begin{aligned} A_{nm}(\boldsymbol{k}) &\to A_{nm}(\boldsymbol{k} - \frac{g\mu_B}{\hbar c}\boldsymbol{A}_{\text{eff},n}), \\ B_{nm}(\boldsymbol{k}) &\to B_{nm}(\boldsymbol{k} - \frac{g\mu_B}{\hbar c}\boldsymbol{A}_{\text{eff},n}). \end{aligned} \tag{A22}$$

While the matrix C_{nm} is unchanged since for which the magnon hopping is not involved.

Now we consider two special cases: the collinear ferromagnet and collinear antiferromagnet. For ferromagnet due to the absence of the magnon paring $a^\dagger_{i,n}a^\dagger_{j,m}$ and $a_{i,n}a_{j,m}$, the 2N dimensional basis is reduce to N dimensional $\Psi^\dagger_{\boldsymbol{k}} = (a^\dagger_{\boldsymbol{k},1}, \cdots a^\dagger_{\boldsymbol{k},N})$. Accordingly, the Hamiltonian Eq. (A10) is reduced to $\mathcal{H}_{\boldsymbol{k}} = A(\boldsymbol{k}) - C$. It is obvious that the global coordinates is same to the local coordinate for each spin, which can be chosen as that where z-direction is identical to the magnetization direction. With this assignment, the magnetic moment of magnon is $-\hbar\hat{\boldsymbol{e}}_z$, and the effective vector potential is $\boldsymbol{A}_{\text{eff}} = \boldsymbol{A}_{\text{eff},n} = \frac{1}{c}\boldsymbol{E}\times\hat{\boldsymbol{e}}_z$. Consequently, the kernal Hamiltonian becomes $\mathcal{H}(\boldsymbol{k}) = A(\boldsymbol{k} - \frac{g\mu_B}{\hbar c}\boldsymbol{A}_{\text{eff}}) - C$.

However, it takes a few steps more to apply Eq. (A21) to antiferromagnet. To be concrete, we consider a collinear antiferromagnet honeycomb lattice as a paradigm. It has two spins in a unit cell, with the Hamiltonian given by

$$H = J_1\sum_{\langle i,j\rangle}\boldsymbol{S}_i\cdot\boldsymbol{S}_j + D\sum_{\langle\langle ij\rangle\rangle}\xi_{ij}\hat{\boldsymbol{z}}\cdot\boldsymbol{S}_i\times\boldsymbol{S}_j + K\sum_i S^2_{iz}. \tag{A23}$$

In which $J_1 > 0$ is the antiferromagnetic exchange interaction, D is the DMI interaction along the z direction, and $\xi_{ij} = 1(-1)$ when $\boldsymbol{S}_i$ and $\boldsymbol{S}_j$ are arranged in a counterclockwise (clockwise) manner. $K < 0$ is the easy axis anisotropy. One can choose the local coordinates of 1st spin of the unit cell as the global coordinates, while the local coordinates of the 2nd spin is obtained by a π rotation about the x-axis or y-axis of the global coordinates. subsequently, the HP transformation is preformed as

$$\begin{aligned} \boldsymbol{S}^\alpha_{i,1} &= \sqrt{\frac{S}{2}}\hat{\boldsymbol{u}}_1 a_{i,1} + \sqrt{\frac{S}{2}}\hat{\boldsymbol{u}}^*_1 a^\dagger_{i,1} + \hat{\boldsymbol{z}}_1(S - a^\dagger_{i,1}a_{i,1}), \\ \boldsymbol{S}^\alpha_{i,2} &= \sqrt{\frac{S}{2}}\hat{\boldsymbol{u}}_2 a_{i,2} + \sqrt{\frac{S}{2}}\hat{\boldsymbol{u}}^*_2 a^\dagger_{i,2} + \hat{\boldsymbol{z}}_2(S - a^\dagger_{i,2}a_{i,2}), \end{aligned} \tag{A24}$$

In which

$$\begin{aligned} &\begin{pmatrix} u^x_1 \\ u^y_1 \\ u^z_1 \end{pmatrix} = \begin{pmatrix} 1 \\ -i \\ 0 \end{pmatrix}, \quad \begin{pmatrix} z^x_1 \\ z^y_1 \\ z^z_1 \end{pmatrix} = \begin{pmatrix} 0 \\ 0 \\ 1 \end{pmatrix}, \\ &\begin{pmatrix} u^x_2 \\ u^y_2 \\ u^z_2 \end{pmatrix} = \begin{pmatrix} 1 \\ i \\ 0 \end{pmatrix}, \quad \begin{pmatrix} z^x_2 \\ z^y_2 \\ z^z_2 \end{pmatrix} = \begin{pmatrix} 0 \\ 0 \\ -1 \end{pmatrix}. \end{aligned} \tag{A25}$$

Therefore the magnon Hamiltonian is $H = H_J + H_D + H_K$ with

$$\begin{aligned}H_J =& J_1 S \sum_{\langle i,j\rangle}(a_{i,1}a_{j,2} + a_{i,1}^\dagger a_{j,2}^\dagger),\\ H_D =& -\sum_{\langle\langle i,j\rangle\rangle} iD_2 S(a_{i,1}^\dagger a_{j,1} - a_{j,1}^\dagger a_{i,1} - a_{i,2}^\dagger a_{j,2} + a_{j,2}^\dagger a_{i,2}),\\ H_K =& \sum_i (3J_1 - K)S(a_{i,1}^\dagger a_{i,1} + a_{i,2}^\dagger a_{i,2}).\end{aligned} \tag{A26}$$

The operator $a_{i,1}$ ($a_{i,1}^\dagger$) annihilates (creates) a magnon with magnetic moment $-\hbar\hat{\boldsymbol{e}}_z$, and the effective vector potential is given as $\boldsymbol{A}_{\text{eff},n} = \boldsymbol{A}_{\text{eff}} = \frac{1}{c}\boldsymbol{E}\times\boldsymbol{e}_z$. The magnon Hamiltonian in the presence of the electric field is written as

$$\begin{aligned}H_J =& J_1 S\sum_{i,\delta}(a_{i,1}a_{i+\delta,2}e^{i\theta^N_{r_i,r_i+\delta}} + \text{h.c.}),\\ H_D =& -\sum_{i,\vartheta} iD_2 S(a_{i,1}^\dagger a_{i+\vartheta,1}e^{-i\theta^{NN}_{r_i,r_i+\vartheta}}\\ &- a_{i,2}^\dagger a_{i+\vartheta,2}e^{i\theta^{NN}_{r_i,r_i+\vartheta}} + \text{h.c.}),\end{aligned} \tag{A27}$$

where the phase accumulated along the nearest (second-nearest) neighbor hopping is given as

$$\begin{aligned}\theta^N_{r_i,r_i+\delta} =& -\frac{g\mu_B}{\hbar c^2}\int_{r_i}^{r_i+\delta}(\boldsymbol{E}(t)\times\boldsymbol{e}_z)\cdot d\boldsymbol{r},\\ \theta^{NN}_{r_i,r_i+\vartheta} =& -\frac{g\mu_B}{\hbar c^2}\int_{r_i}^{r_i+\vartheta}(\boldsymbol{E}(t)\times\boldsymbol{e}_z)\cdot d\boldsymbol{r}.\end{aligned} \tag{A28}$$

Supposing that the scale of the spacial variance of $\boldsymbol{E}$ is much larger than lattice constant one obtains

$$\begin{aligned}\theta^N_{r_i,r_i+\delta} =& \frac{g\mu_B}{\hbar c}\boldsymbol{A}_{\text{eff}}\cdot\boldsymbol{\delta},\\ \theta^{NN}_{r_i,r_i+\vartheta} =& \frac{g\mu_B}{\hbar c}\boldsymbol{A}_{\text{eff}}\cdot\boldsymbol{\vartheta}.\end{aligned} \tag{A29}$$

Making use of the Fourier transformation Eq. (A9), one directly obtains $H = \sum_{\boldsymbol{k}}\Psi^\dagger_{\boldsymbol{k}}\mathcal{H}(\boldsymbol{k} - \frac{g\mu_B}{\hbar c}\boldsymbol{A}_{\text{eff}})\Psi_{\boldsymbol{k}}$, with the Nambu basis given by $\Psi^\dagger_{\boldsymbol{k}} = (a^\dagger_{\boldsymbol{k},1}, a^\dagger_{\boldsymbol{k},2}, a_{-\boldsymbol{k},1}, a_{-\boldsymbol{k},2})$. In which $A_{mn}(\boldsymbol{k}) - C_{mn}$ is diagonal with $A_{11(22)}(\boldsymbol{k}) - C_{11(22)} = \frac{S}{2}\left[3J_1 - K(2S-1)/S \pm D\sum_{\boldsymbol{\delta}}2\sin(\boldsymbol{k}\cdot\boldsymbol{\delta})\right]$, and $B_{mn}(\boldsymbol{k})$ is non-diagonal with $B_{12}(\boldsymbol{k}) = B^*_{21}(\boldsymbol{k}) = \frac{S}{2}\left[\sum_{\boldsymbol{\vartheta}}\exp(i\boldsymbol{k}\cdot\boldsymbol{\vartheta})\right]$.

Appendix B: Gauge transformation and dipole interaction

In this section we give a gauge transformation to derive perturbed Hamiltonian in form of a dipole interaction. The single-particle Hamiltonian and the Bloch Hamiltonian satisfy

$$\mathcal{H}_0(-i\boldsymbol{\nabla}, \boldsymbol{r}) = e^{i\boldsymbol{k}\cdot\boldsymbol{r}}\mathcal{H}_0(\boldsymbol{k})e^{-i\boldsymbol{k}\cdot\boldsymbol{r}}, \tag{B1}$$

then the perturbed Hamiltonian is written as

$$\mathcal{H}_A = \mathcal{H}_0\left(-i\boldsymbol{\nabla} + \frac{g\mu_B}{\hbar c}\boldsymbol{A}_{\text{eff}}, \boldsymbol{r}\right) \tag{B2}$$

The time-dependent Schördinger equation is

$$i\hbar\frac{\partial\left|\psi(\boldsymbol{r},t)\right\rangle}{\partial t} = \mathcal{H}_A\left|\psi(\boldsymbol{r},t)\right\rangle. \tag{B3}$$

A unitary gauge transformation of $|\psi(\boldsymbol{r},t)\rangle$ takes the form

$$\left|\psi'(\boldsymbol{r},t)\right\rangle = \mathcal{U}(t)\left|\psi(\boldsymbol{r},t)\right\rangle, \tag{B4}$$

The time-dependent Schördinger equation transforms as

$$\begin{aligned}&i\hbar\frac{\partial\left|\psi'(\boldsymbol{r},t)\right\rangle}{\partial t}\\ &= \left[\mathcal{U}\mathcal{H}_A\mathcal{U}^\dagger\left|\psi(\boldsymbol{r},t)\right\rangle + i\hbar\frac{\partial\mathcal{U}(t)}{\partial t}\mathcal{U}^\dagger(t)\right]\left|\psi'(\boldsymbol{r},t)\right\rangle.\end{aligned} \tag{B5}$$

If the unitary transformation is chosen as $\mathcal{U}(t) = e^{i\mathcal{K}(t)}$ with

$$\mathcal{K}(t) = \frac{g\mu_B}{\hbar c}\boldsymbol{A}_{\text{eff}}(t)\cdot\boldsymbol{r}. \tag{B6}$$

For the first term in the r.h.s. of Eq. (B5), by use of the Baker-Campbell-Hausdorff identity

$$\begin{aligned}e^{i\mathcal{K}}\mathcal{H}_A e^{-i\mathcal{K}} =& \mathcal{H} + i[\mathcal{K},\mathcal{H}_A] - \frac{1}{2}[\mathcal{K},[\mathcal{K},\mathcal{H}_A]] + ...\\ &+ \frac{i^n}{n!}[\mathcal{K},...,[\mathcal{K},\mathcal{H}_A]] + ...,\end{aligned} \tag{B7}$$

it is obtained that

$$\mathcal{U}(t)\mathcal{H}_A\mathcal{U}^\dagger(t) = \mathcal{H}_0. \tag{B8}$$

For the second term in the r.h.s. of Eq. (B5), by introducing the effective electric field $\boldsymbol{\mathcal{E}} = -\partial_t\boldsymbol{A}_{\text{eff}}$, it is straightforward to show that

$$i\hbar\frac{\partial\mathcal{U}(t)}{\partial t}\mathcal{U}^\dagger(t) = \frac{g\mu_B}{c}\boldsymbol{\mathcal{E}}(t)\cdot\boldsymbol{r}. \tag{B9}$$

Then the Hamiltonian in velocity gauge transform to

$$\mathcal{H}_E(t) = \mathcal{H}_0(\boldsymbol{k}) + \frac{g\mu_B}{c}\boldsymbol{\mathcal{E}}(t)\cdot\boldsymbol{r}. \tag{B10}$$

This coincides with Eq. (4).

Appendix C: Dynamical and geometric phase in tunnelling process

By inserting Eq. (7) into the time-dependent Schördinger equation Eq. (6), we have

$$\sum_m e^{-i\int_{t_0}^t dt_1\left[\varepsilon_m+\frac{g\mu_B}{c}\boldsymbol{\mathcal{E}}(t)\cdot\boldsymbol{\mathcal{A}}_{mm}\right]/\hbar}\left(i\hbar\partial_t C_{lm}(t)+\frac{g\mu_B}{c}\boldsymbol{\mathcal{E}}\cdot\boldsymbol{\mathcal{A}}_{mm}C_{lm}(t)-\frac{g\mu_B}{c}C_{lm}(t)\boldsymbol{\mathcal{E}}\cdot\nabla_{\boldsymbol{k}}\right)|m,\boldsymbol{k}(t)\rangle=0, \tag{C1}$$

where we use

$$\hbar\partial_t\,|m,\boldsymbol{k}(t)\rangle=\frac{g\mu_B}{c}\boldsymbol{\mathcal{E}}\cdot\nabla_{\boldsymbol{k}}\,|m,\boldsymbol{k}(t)\rangle\,. \tag{C2}$$

Taking an inner product with $\langle m,\boldsymbol{k}(t)|$ for Eq. (C1), we have

$$\begin{aligned}
i\partial_t C_{ln}(t)=&\frac{g\mu_B}{\hbar c}\sum_{m\neq n}\boldsymbol{\mathcal{E}}\cdot\boldsymbol{\mathcal{A}}_{nm}e^{i\int_{t_0}^t dt_1\left[\varepsilon_n+\frac{g\mu_B}{c}\boldsymbol{\mathcal{E}}(t)\cdot\mathcal{A}_{nn}\right]/\hbar}e^{-i\int_{t_0}^t dt_1\left[\varepsilon_m+\frac{g\mu_B}{c}\boldsymbol{\mathcal{E}}(t)\cdot\boldsymbol{\mathcal{A}}_{mm}\right]/\hbar}C_{lm}(t)\\
=&\frac{g\mu_B}{\hbar c}\mathcal{E}^\alpha|\mathcal{A}^\alpha_{nm}|e^{i\int_{t_0}^t dt_1\left[\varepsilon_n-\varepsilon_m+\frac{g\mu_B}{c}\mathcal{E}^\beta(t)\cdot(\mathcal{A}^\beta_{nn}-\mathcal{A}^\beta_{mm})\right]/\hbar+i\arg\mathcal{A}^\alpha_{nm}(t)}C_{lm}(t)\\
=&\frac{g\mu_B}{\hbar c}\mathcal{E}^\alpha|\mathcal{A}^\alpha_{nm}|e^{i\int_{t_0}^t dt_1\left[\varepsilon_n-\varepsilon_m+\frac{g\mu_B}{c}\mathcal{E}^\beta(t)\cdot(\mathcal{A}^\beta_{nn}-\mathcal{A}^\beta_{mm})+\hbar\partial_t\arg\mathcal{A}^\alpha_{nm}\right]/\hbar+i\arg\mathcal{A}^\alpha_{nm}(t_0)}C_{lm}(t).
\end{aligned} \tag{C3}$$

which results to Eq. (9).

Appendix D: Derivation of the magnon spin current

Now we define the magnon spin current. Because the z component of the total spin is conserved, The local magnon momentum density is $\hat{n}_z(\boldsymbol{r}_i)=\hbar\sum_m \boldsymbol{z}_m a^\dagger_{i,m}a_{i,m}$ satisfies the continuity equation. The Fourier transformation of the local magnon density is written as

$$\hat{n}_z(\boldsymbol{r}_i)=\frac{\hbar}{N}\sum_{\boldsymbol{kq}m}\boldsymbol{z}_m e^{-i\boldsymbol{q}\cdot(\boldsymbol{r}_i+\boldsymbol{t}_m)}a^\dagger_{\boldsymbol{k}+\boldsymbol{q},m}a_{\boldsymbol{k},m}. \tag{D1}$$

The Heisenberg equation of motion for $a_{\boldsymbol{k},m}$ is used to derive the equation of motion for $n_z(\boldsymbol{r}_i)$:

$$\begin{aligned}
\dot{a}_{\boldsymbol{k},m}=&\frac{1}{i\hbar}[a_{\boldsymbol{k},m},H]\\
=&\frac{1}{i\hbar}\sum_n(A_{\boldsymbol{k},mn}a_{\boldsymbol{k},n}+A_{\boldsymbol{k},mn}a_{\boldsymbol{k},n}+B^*_{\boldsymbol{k},mn}a_{-\boldsymbol{k},n}),\\
=&\frac{1}{i\hbar}\sum_n(2A_{\boldsymbol{k},mn}a_{\boldsymbol{k},n}+B_{\boldsymbol{k},mn}a^\dagger_{-\boldsymbol{k},n}+B_{-\boldsymbol{k},nm}a^\dagger_{-\boldsymbol{k},n}),
\end{aligned} \tag{D2}$$

where H is given by Eq. (A10), and we obtain:

$$\begin{aligned}
&\frac{\partial\hat{n}_z(\boldsymbol{r}_i)}{\partial t}\\
=&\frac{1}{iN}\sum_{\boldsymbol{kq}mn}e^{-i\boldsymbol{q}\cdot\boldsymbol{r}_{i,m}}\boldsymbol{z}_m\Big[-(2A_{\boldsymbol{k}+\boldsymbol{q},nm}a^\dagger_{\boldsymbol{k}+\boldsymbol{q},n}\\
&+(B^*_{\boldsymbol{k}+\boldsymbol{q},mn}+B^*_{-\boldsymbol{k}-\boldsymbol{q},nm})a^\dagger_{-\boldsymbol{k}-\boldsymbol{q},n})a_{\boldsymbol{k},m}\\
&+a^\dagger_{\boldsymbol{k}+\boldsymbol{q},m}(2A_{\boldsymbol{k},mn}a_{\boldsymbol{k},n}+(B_{\boldsymbol{k},mn}+B_{-\boldsymbol{k},nm})a^\dagger_{-\boldsymbol{k},n})\Big].
\end{aligned} \tag{D3}$$

In the case $\sum\boldsymbol{\delta}=0$ and assuming the long-wavelength limit $\boldsymbol{q}\to 0$, the magnon spin current is obtained by use of the continuity equation $\partial n_{z\boldsymbol{q}}/\partial t+i\boldsymbol{q}\cdot\boldsymbol{J}^s_z=0$, which is given as

$$\begin{aligned}
\hat{\boldsymbol{J}}^s_z=&\sum_{\boldsymbol{k}mn}\boldsymbol{z}_m\Bigg(\frac{\partial A_{\boldsymbol{k},mn}}{\partial\boldsymbol{k}}a^\dagger_{\boldsymbol{k},m}a_{\boldsymbol{k},n}+\frac{\partial A_{-\boldsymbol{k},nm}}{\partial\boldsymbol{k}}a_{-\boldsymbol{k},m}a^\dagger_{-\boldsymbol{k},n}\\
&+\frac{\partial B_{\boldsymbol{k},mn}}{\partial\boldsymbol{k}}a^\dagger_{\boldsymbol{k},m}a^\dagger_{-\boldsymbol{k},n}+\frac{\partial B^*_{\boldsymbol{k},nm}}{\partial\boldsymbol{k}}a_{-\boldsymbol{k},m}a_{\boldsymbol{k},n}\Bigg)\\
=&\hbar\sum_{\boldsymbol{k}}\Psi^\dagger_{\boldsymbol{k}}\mathcal{Z}\frac{\partial\mathcal{H}_{\boldsymbol{k}}}{\partial\boldsymbol{k}}\Psi_{\boldsymbol{k}}.
\end{aligned} \tag{D4}$$

In Eq. (D4) we define the diagonal matrix $\mathcal{Z}$

$$\mathcal{Z}=\mathrm{diag}(z_1,\cdots,z_m,z_1,\cdots,z_m). \tag{D5}$$

Making use of Eq. (A18), we have $\hat{\boldsymbol{J}}^s_z=\sum_{\boldsymbol{k}}\hat{\boldsymbol{J}}^s_{\boldsymbol{k},z}$ with

$$\hat{\boldsymbol{J}}^s_{\boldsymbol{k},z}=\Phi^\dagger_{\boldsymbol{k}}\Sigma_z\widetilde{\frac{\partial\mathcal{Z}\mathcal{H}_{\boldsymbol{k}}}{\partial\boldsymbol{k}}}\Phi_{\boldsymbol{k}}. \tag{D6}$$

It is found that

$$\widetilde{\frac{\partial\mathcal{Z}\mathcal{H}_{\boldsymbol{k}}}{\partial\boldsymbol{k}}}=\frac{\partial\widetilde{\mathcal{Z}\mathcal{H}_{\boldsymbol{k}}}}{\partial\boldsymbol{k}}-\widetilde{\mathcal{Z}\mathcal{H}_{\boldsymbol{k}}}U^{-1}_{\boldsymbol{k}}\frac{\partial U_{\boldsymbol{k}}}{\partial\boldsymbol{k}}-\frac{\partial U^{-1}_{\boldsymbol{k}}}{\partial\boldsymbol{k}}U_{\boldsymbol{k}}\widetilde{\mathcal{Z}\mathcal{H}_{\boldsymbol{k}}}, \tag{D7}$$

and we obtain

$$\hat{\boldsymbol{J}}^s_{\boldsymbol{k},z}=\Phi^\dagger_{\boldsymbol{k}}\Sigma_z\left(\frac{\partial\widetilde{\mathcal{Z}\mathcal{H}_{\boldsymbol{k}}}}{\partial\boldsymbol{k}}-i[\boldsymbol{\mathcal{A}}_{\boldsymbol{k}},\widetilde{\mathcal{Z}\mathcal{H}_{\boldsymbol{k}}}]\right)\Phi_{\boldsymbol{k}}, \tag{D8}$$

where the Berry connection is defined by

$$\boldsymbol{\mathcal{A}}_{\boldsymbol{k}}=iU^{-1}_{\boldsymbol{k}}\frac{\partial U_{\boldsymbol{k}}}{\partial\boldsymbol{k}}=i\Sigma_z U^\dagger_{\boldsymbol{k}}\Sigma_z\frac{\partial U_{\boldsymbol{k}}}{\partial\boldsymbol{k}}. \tag{D9}$$

Noting that the Berry connection given in Eq. (D9) is different from $iU^\dagger_{\boldsymbol{k}}\frac{\partial U_{\boldsymbol{k}}}{\partial\boldsymbol{k}}$. This is because that the Bogoliubov transformation is generally not unitary [58]. For ferromagnets $\mathcal{Z}$ is unit matrix and we have

$$\hat{\boldsymbol{J}}^s_{\boldsymbol{k},z}=\Phi^\dagger_{\boldsymbol{k}}\left(\frac{\partial\mathcal{H}_{\boldsymbol{k}}}{\partial\boldsymbol{k}}-i[\boldsymbol{\mathcal{A}}_{\boldsymbol{k}},\mathcal{H}_{\boldsymbol{k}}]\right)\Phi_{\boldsymbol{k}}. \tag{D10}$$

Making use of Eq. (7), we have

$$\langle \Psi_m, \boldsymbol{k}_0(t) | \hat{J}^s_{\boldsymbol{k}_0,z} | \Psi_m, \boldsymbol{k}_0(t) \rangle = \sum_n \nabla_{\boldsymbol{k}_0} \varepsilon_n |C_{mn\boldsymbol{k}_0}(t)|^2 - \left(i \sum_n \varepsilon_{mn} \boldsymbol{\mathcal{A}}_{nm}(\boldsymbol{k}_0(t)) C^*_{mn\boldsymbol{k}_0}(t) C_{mm\boldsymbol{k}_0}(t) + \text{h.c.} \right). \tag{D11}$$

Making use of the property

$$0 = \nabla_{\boldsymbol{k}_0} \langle \Psi_m, \boldsymbol{k}_0(t) | \Psi_m, \boldsymbol{k}_0(t) \rangle = \sum_n C^*_{mn\boldsymbol{k}_0} \nabla_{\boldsymbol{k}_0} C_{mn\boldsymbol{k}_0} + \sum_n \langle u_n, \boldsymbol{k}(t) | \nabla_{\boldsymbol{k}_0} | u_m, \boldsymbol{k}(t) \rangle C^*_{mn\boldsymbol{k}_0} C_{mm\boldsymbol{k}_0} + \text{h.c.}, \tag{D12}$$

we have

$$-\sum_n i C^*_{mn\boldsymbol{k}_0} \nabla_{\boldsymbol{k}_0} C_{mn\boldsymbol{k}_0} = \sum_n \boldsymbol{\mathcal{A}}_{nm}(\boldsymbol{k}_0(t)) C^*_{mn\boldsymbol{k}_0} C_{mm\boldsymbol{k}_0}. \tag{D13}$$

Inserting Eq. (D13) into Eq. (D11), we have

$$\begin{aligned}
&\langle \Psi_m, \boldsymbol{k}_0(t) | \hat{J}^s_{\boldsymbol{k}_0,z} | \Psi_m, \boldsymbol{k}_0(t) \rangle \\
=& \sum_n \nabla_{\boldsymbol{k}_0} \varepsilon_n |C_{mn\boldsymbol{k}_0}(t)|^2 - \left(\sum_n \varepsilon_{mn} C^*_{mn\boldsymbol{k}_0} \nabla_{\boldsymbol{k}_0} C_{mn\boldsymbol{k}_0} + \text{h.c.}. \right) \\
=& \sum_n \nabla_{\boldsymbol{k}_0} \varepsilon_n |C_{mn\boldsymbol{k}_0}(t)|^2 - \varepsilon_{mn} \nabla_{\boldsymbol{k}_0} P_{mn\boldsymbol{k}_0} \\
=& -\nabla_{\boldsymbol{k}_0} (\varepsilon_{mn} P_{mn\boldsymbol{k}_0}).
\end{aligned} \tag{D14}$$

This coincides with Eq. (14).

[1] C. Kittel, *Introduction to solid state physics* (John Wiley & sons, inc, 2005).

[2] V. V. Kruglyak, S. O. Demokritov, and D. Grundler, Magnonics, Journal of Physics D: Applied Physics **43**, 264001 (2010).

[3] Y. Kajiwara, K. Harii, S. Takahashi, J.-i. Ohe, K. Uchida, M. Mizuguchi, H. Umezawa, H. Kawai, K. Ando, K. Takanashi, *et al.*, Transmission of electrical signals by spin-wave interconversion in a magnetic insulator, Nature **464**, 262 (2010).

[4] A. V. Chumak, V. I. Vasyuchka, A. A. Serga, and B. Hillebrands, Magnon spintronics, Nat. Phys. **11**, 453 (2015).

[5] V. Baltz, A. Manchon, M. Tsoi, T. Moriyama, T. Ono, and Y. Tserkovnyak, Antiferromagnetic spintronics, Rev. Mod. Phys. **90**, 015005 (2018).

[6] T. Jungwirth, J. Sinova, A. Manchon, X. Marti, J. Wunderlich, and C. Felser, The multiple directions of antiferromagnetic spintronics, Nat. Phys. **14**, 200 (2018).

[7] J. Xiao, G. E. W. Bauer, K.-c. Uchida, E. Saitoh, and S. Maekawa, Theory of magnon-driven spin seebeck effect, Phys. Rev. B **81**, 214418 (2010).

[8] S. M. Rezende, R. L. Rodríguez-Suárez, R. O. Cunha, A. R. Rodrigues, F. L. A. Machado, G. A. Fonseca Guerra, J. C. Lopez Ortiz, and A. Azevedo, Magnon spin-current theory for the longitudinal spin-seebeck effect, Phys. Rev. B **89**, 014416 (2014).

[9] S. Seki, T. Ideue, M. Kubota, Y. Kozuka, R. Takagi, M. Nakamura, Y. Kaneko, M. Kawasaki, and Y. Tokura, Thermal generation of spin current in an antiferromagnet, Phys. Rev. Lett. **115**, 266601 (2015).

[10] S. M. Wu, W. Zhang, A. KC, P. Borisov, J. E. Pearson, J. S. Jiang, D. Lederman, A. Hoffmann, and A. Bhattacharya, Antiferromagnetic spin seebeck effect, Phys. Rev. Lett. **116**, 097204 (2016).

[11] H. Katsura, N. Nagaosa, and P. A. Lee, Theory of the thermal hall effect in quantum magnets, Phys. Rev. Lett. **104**, 066403 (2010).

[12] Y. Onose, T. Ideue, H. Katsura, Y. Shiomi, N. Nagaosa, and Y. Tokura, Observation of the magnon hall effect, Science **329**, 297 (2010).

[13] R. Matsumoto and S. Murakami, Theoretical prediction of a rotating magnon wave packet in ferromagnets, Phys. Rev. Lett. **106**, 197202 (2011).

[14] R. Cheng, S. Okamoto, and D. Xiao, Spin nernst effect of magnons in collinear antiferromagnets, Phys. Rev. Lett. **117**, 217202 (2016).

[15] V. A. Zyuzin and A. A. Kovalev, Magnon spin nernst effect in antiferromagnets, Phys. Rev. Lett. **117**, 217203 (2016).

[16] Y. Shiomi, R. Takashima, and E. Saitoh, Experimental evidence consistent with a magnon nernst effect in the antiferromagnetic insulator $mnps_3$, Phys. Rev. B **96**, 134425 (2017).

[17] B. Li, S. Sandhoefner, and A. A. Kovalev, Intrinsic spin nernst effect of magnons in a noncollinear antiferromagnet, Phys. Rev. Res. **2**, 013079 (2020).

[18] Z. Du, H.-Z. Lu, and X. Xie, Nonlinear hall effects, Nature Reviews Physics **3**, 744 (2021).

[19] Y. Wang, Z.-G. Zhu, and G. Su, Quantum theory of nonlinear thermal response, Phys. Rev. B **106**, 035148 (2022).

[20] H. Kondo and Y. Akagi, Nonlinear magnon spin nernst effect in antiferromagnets and strain-tunable pure spin

current, Phys. Rev. Res. **4**, 013186 (2022).
[21] E. V. n. Boström, T. S. Parvini, J. W. McIver, A. Rubio, S. V. Kusminskiy, and M. A. Sentef, All-optical generation of antiferromagnetic magnon currents via the magnon circular photogalvanic effect, Phys. Rev. B **104**, L100404 (2021).
[22] I. Kézsmárki, N. Kida, H. Murakawa, S. Bordács, Y. Onose, and Y. Tokura, Enhanced directional dichroism of terahertz light in resonance with magnetic excitations of the multiferroic $ba_2coge_2o_7$ oxide compound, Phys. Rev. Lett. **106**, 057403 (2011).
[23] Y. Takahashi, R. Shimano, Y. Kaneko, H. Murakawa, and Y. Tokura, Magnetoelectric resonance with electromagnons in a perovskite helimagnet, Nat. Phys. **8**, 121 (2012).
[24] S. Bordács, I. Kézsmárki, D. Szaller, L. Demkó, N. Kida, H. Murakawa, Y. Onose, R. Shimano, T. Room, U. Nagel, *et al.*, Chirality of matter shows up via spin excitations, Nat. Phys. **8**, 734 (2012).
[25] K. Fujiwara, S. Kitamura, and T. Morimoto, Nonlinear spin current of photoexcited magnons in collinear antiferromagnets, Phys. Rev. B **107**, 064403 (2023).
[26] Y. Aharonov and A. Casher, Topological quantum effects for neutral particles, Phys. Rev. Lett. **53**, 319 (1984).
[27] L. D. Landau and E. M. Lifshitz, *Quantum mechanics: non-relativistic theory*, Vol. 3 (Elsevier, 2013).
[28] C. Zener, Non-adiabatic crossing of energy levels, Proc. R. Soc. Lond. Ser. A. **137**, 696 (1932).
[29] M. V. Berry, Geometric amplitude factors in adiabatic quantum transitions, Proc. R. Soc. Lond. Ser. A. **430**, 405 (1990).
[30] A. Joye, H. Kunz, and C.-E. Pfister, Exponential decay and geometric aspect of transition probabilities in the adiabatic limit, Annals Phys. **208**, 299 (1991).
[31] B. Wu and Q. Niu, Nonlinear landau-zener tunneling, Phys. Rev. A **61**, 023402 (2000).
[32] J. Liu, L. Fu, B.-Y. Ou, S.-G. Chen, D.-I. Choi, B. Wu, and Q. Niu, Theory of nonlinear landau-zener tunneling, Phys. Rev. A **66**, 023404 (2002).
[33] E. P. Glasbrenner and W. P. Schleich, The landau–zener formula made simple, J. Phys. B: At. Mol. Opt. Phys. **56**, 104001 (2023).
[34] V. Ivakhnenko, S. N. Shevchenko, and F. Nori, Nonadiabatic landau–zener–stückelberg–majorana transitions, dynamics, and interference, Phys. Rep. **995**, 1 (2023).
[35] S. Kitamura, N. Nagaosa, and T. Morimoto, Current response of nonequilibrium steady states in the landau-zener problem: Nonequilibrium green's function approach, Phys. Rev. B **102**, 245141 (2020).
[36] S. Kitamura, N. Nagaosa, and T. Morimoto, Nonreciprocal landau–zener tunneling, Commun. Phys. **3**, 63 (2020).
[37] S. Takayoshi, J. Wu, and T. Oka, Nonadiabatic nonlinear optics and quantum geometry — Application to the twisted Schwinger effect, SciPost Phys. **11**, 075 (2021).
[38] Y. Suzuki, Tunneling spin current in systems with spin degeneracy, Phys. Rev. B **105**, 075201 (2022).
[39] R. Mignani, Aharonov-casher effect and geometrical phases, Journal of Physics A: Mathematical and General **24**, L421 (1991).
[40] F. Meier and D. Loss, Magnetization transport and quantized spin conductance, Phys. Rev. Lett. **90**, 167204 (2003).
[41] K. Nakata, S. K. Kim, J. Klinovaja, and D. Loss, Magnonic topological insulators in antiferromagnets, Phys. Rev. B **96**, 224414 (2017).
[42] K. Nakata, J. Klinovaja, and D. Loss, Magnonic quantum hall effect and wiedemann-franz law, Phys. Rev. B **95**, 125429 (2017).
[43] Y. Wang, Z.-G. Zhu, and G. Su, Magnon spin photogalvanic effect in collinear ferromagnets, arXiv preprint arXiv:2307.10882 https://doi.org/10.48550/arXiv.2307.10882 (2023).
[44] J. E. Sipe and A. I. Shkrebtii, Second-order optical response in semiconductors, Phys. Rev. B **61**, 5337 (2000).
[45] S. M. Young and A. M. Rappe, First principles calculation of the shift current photovoltaic effect in ferroelectrics, Phys. Rev. Lett. **109**, 116601 (2012).
[46] A. M. Cook, B. M. Fregoso, F. De Juan, S. Coh, and J. E. Moore, Design principles for shift current photovoltaics, Nat. Commun. **8**, 14176 (2017).
[47] P.-T. Wei, J.-Y. Ni, X.-M. Zheng, D.-Y. Liu, and L.-J. Zou, Topological magnons in one-dimensional ferromagnetic su–schrieffer–heeger model with anisotropic interaction, J. Condens. Matter Phys. **34**, 495801 (2022).
[48] G. L. J. A. Rikken and P. Wyder, Magnetoelectric anisotropy in diffusive transport, Phys. Rev. Lett. **94**, 016601 (2005).
[49] F. Pop, P. Auban-Senzier, E. Canadell, G. L. Rikken, and N. Avarvari, Electrical magnetochiral anisotropy in a bulk chiral molecular conductor, Nat. Commun. **5**, 3757 (2014).
[50] R. Wakatsuki, Y. Saito, S. Hoshino, Y. M. Itahashi, T. Ideue, M. Ezawa, Y. Iwasa, and N. Nagaosa, Nonreciprocal charge transport in noncentrosymmetric superconductors, Science Advances **3**, e1602390 (2017).
[51] Y. Iguchi, S. Uemura, K. Ueno, and Y. Onose, Nonreciprocal magnon propagation in a noncentrosymmetric ferromagnet $life_5o_8$, Phys. Rev. B **92**, 184419 (2015).
[52] G. Gitgeatpong, Y. Zhao, P. Piyawongwatthana, Y. Qiu, L. W. Harriger, N. P. Butch, T. J. Sato, and K. Matan, Nonreciprocal magnons and symmetry-breaking in the noncentrosymmetric antiferromagnet, Phys. Rev. Lett. **119**, 047201 (2017).
[53] T. J. Sato and K. Matan, Nonreciprocal magnons in noncentrosymmetric magnets, J. Phys. Soc. Jpn. **88**, 081007 (2019).
[54] P. Němec, M. Fiebig, T. Kampfrath, and A. V. Kimel, Antiferromagnetic opto-spintronics, Nat. Phys. **14**, 229 (2018).
[55] S. Petit, Numerical simulations and magnetism, École thématique de la Société Française de la Neutronique **12**, 105 (2011).
[56] S. Toth and B. Lake, Linear spin wave theory for single-q incommensurate magnetic structures, J. Condens. Matter Phys. **27**, 166002 (2015).
[57] R. Shindou, R. Matsumoto, S. Murakami, and J.-i. Ohe, Topological chiral magnonic edge mode in a magnonic crystal, Phys. Rev. B **87**, 174427 (2013).
[58] M.-w. Xiao, Theory of transformation for the diagonalization of quadratic hamiltonians, arXiv preprint arXiv:0908.0787 https://doi.org/10.48550/arXiv.0908.0787 (2009).